Journal Pre-proof

Detailed Study of Collagen, Vasculature, and Innervation in the Human Cardiac Conduction System

Denis Depes , Ari Mennander , Timo Paavonen ,
Mary N. Sheppard , Ivana Kholová

Please cite this article as: Denis Depes , Ari Mennander , Timo Paavonen , Mary N. Sheppard , Ivana Kholová , Detailed Study of Collagen, Vasculature, and Innervation in the Human Cardiac Conduction System, *Cardiovascular Pathology* (2023), doi: https://doi.org/10.1016/j.carpath.2023.107603

This is a PDF file of an article that has undergone enhancements after acceptance, such as the addition of a cover page and metadata, and formatting for readability, but it is not yet the definitive version of record. This version will undergo additional copyediting, typesetting and review before it is published in its final form, but we are providing this version to give early visibility of the article. Please note that, during the production process, errors may be discovered which could affect the content, and all legal disclaimers that apply to the journal pertain.

Highlights

- The morphologic substrates of the human cardiac conduction system (CCS) were studied.
- The vasculature, innervation, and collagen differed between the CCS and surrounding tissue.
- The morphologic differences may play a role in the propagation of electrical signals.
- This study sets a morphological benchmark for further investigation of arrhythmias.

Title: Detailed Study of Collagen, Vasculature, and Innervation in the Human Cardiac Conduction System

Denis Depes, MD [a], Ari Mennander, MD, PhD [a,b], Timo Paavonen, MD, PhD [a,c], Mary N. Sheppard, MD, PhD [d], Ivana Kholová, MD, PhD [a,c]

- [a.] Faculty of Medicine and Health Technology, Tampere University, Arvo Ylpön katu 34, 33520 Tampere, Finland; denis.depes@tuni.fi, timo.paavonen@tuni.fi, ivana.kholova@tuni.fi
- [b.] Division of Cardiothoracic Surgery, Tampere University Heart Hospital, Elämänaukio 1, 33520 Tampere, Finland; ari.mennander@sydansairaala.fi
- [c.] Department of Pathology, Fimlab Laboratories, Arvo Ylpön katu 4, 33520 Tampere, Finland
- [d.] Department of Cardiovascular Pathology, Cardiology Clinical Academic Group, Molecular and Clinical Sciences Research Institute, St George's Medical School, London, United Kingdom; msheppar@sgul.ac.uk

Corresponding author:
Adjunct Professor Ivana Kholová, MD, PhD
Pathology, Fimlab Laboratories
Arvo Ylpön katu 4
33520 Tampere
Finland
ivana.kholova@tuni.fi, +358331174851

Abstract

Background

The cardiac conduction system (CCS) creates and propagates electrical signals generating the heartbeat. This study aimed to assess the collagen content, vasculature, and innervation in the human sinoatrial and atrioventricular CCS, and surrounding tissue.

Materials and Methods

Ten sinoatrial and 17 atrioventricular CCS samples were collected from 17 adult human autopsied hearts. Masson trichrome stain was used to examine collagen, cardiomyocytes, and fat proportions. Immunohistochemically, vessels and lymphatics were studied by CD31 (pan-endothelial marker) and D2-40 (lymphatic endothelium marker) antibodies. General nerve densities were assessed by S100, while sympathetic nerves were studied using tyrosine hydroxylase, parasympathetic nerves with choline acetyltransferase, and GAP43 (neural growth marker) antibodies looked at these components. All components were quantified with QuPath software.

Results

Interstitial collagen was more than two times higher in the sinoatrial vs. atrioventricular CCS (55% vs. 22%). The fat content was 6.3% in the sinoatrial CCS and 6.5% in the atrioventricular CCS. The lymphatic vessel density was increased in the sinoatrial and atrioventricular CCS compared to the surrounding tissue and was lower in the sinoatrial vs. atrioventricular CCS (P=0.043). The overall vasculature density did not differ between the SA and AV CCS. The overall innervation and neural growth densities were significantly increased in the CCS compared to the surrounding tissue. The overall innervation was higher in the atrial vs. ventricular CCS (P=0.018). The neural growth was higher in the atrial vs. ventricular CCS (P=0.018). The sympathetic neural supply was dominant in all the studied regions with the highest density in the sinoatrial CCS.

Conclusions

Our results provide new insights into the unique morphology of the human CCS collagen, fat, vasculature, and innervation. A deeper understanding of the CCS anatomical components and morphologic substrates' role will help in elucidating the causes of cardiac arrhythmias and provide a basis for further therapeutic interventions.

Keywords

human cardiac conduction system, lymphatic vessels, blood vessels, autonomic innervation, interstitial collagen, morphometry

1. Introduction

The cardiac conduction system (CCS) is responsible for initiating and spreading the electric impulse throughout the myocardium resulting in synchronized heart contraction. The CCS consists of the sinoatrial (SA) and atrioventricular (AV) nodes, the bundle of His, bundle branches, and Purkinje fibers [1,2]. Previous histological studies on the CCS morphology have been conducted with disease and age-related changes, but most are very old studies [3–7].

While both replacement and interstitial fibrosis results from the diffuse deposition of collagen in the myocardium and are associated with ventricular dysfunction, arrhythmias, and increased cardiovascular mortality [6], in the SA and AV node collagen is a prominent finding and effectively isolates the specialized cells from the surrounding myocardium preventing unwanted propagation of the electrical impulse [8].

Fat cells can be normally found admixed with myocardial fibers, especially in the right ventricle, and are a normal finding in the human heart [9,10]. Fat infiltration of the conduction tissue has been put forward as a cause of arrhythmias and sudden cardiac death [11–13].

Blood vessels have a vital role in the transportation of oxygen, nutrients, and chemicals to tissues and waste products from tissues; and lymphatic vessels maintain fluid and protein homeostasis. Previous research has found that blood vessels are more numerous than lymphatics in the myocardium [14,15], but no studies investigating the blood and lymphatic vessel distribution and densities in the CCS and its adjacent tissue have been performed.

The autonomic system of the heart, consisting of sympathetic and parasympathetic nerves, extensively innervates the CCS [16]. The distribution of cardiac autonomic nerves was previously studied in different parts of the heart demonstrating an uneven innervation pattern and changes associated with various cardiac conditions [17–20]. Autonomic innervation studied in humans and animals recognized that sympathetic and parasympathetic nerves impacted CCS activity [5,21–26].

This is the latest study, in which we examined the proportions of collagen and fat within the CCS tissue of 17 normal human hearts, as well as general, sympathetic, and parasympathetic nerves and neural growth, and blood and lymphatic vessels.

2. Materials and Methods

2.1 Study Population

The study cohort originated from the CRY cardiac pathology database which has a biobank of 7000 human hearts obtained at autopsy [27]. The SA and AV CCS tissue were dissected from 17 normal hearts (4 females, 13 males). The age ranged from 19 to 70 years, mean age (±SD) was 35.7 ± 15.8 years. The cause of death of all 17 subjects was sudden death, characterized by a morphologically normal heart. The cases had positive lethal toxicology (alcohol or cocaine in most cases). No sudden arrhythmic death syndrome (SADS) was diagnosed.

2.2 Cardiac Conduction System Collection Technique

2.2.1 Sinoatrial Node

Ten SA nodal tissue samples were obtained from the 17 cases. After the right atrium was opened from the inferior vena cava to the right atrial appendage, the location of the SA node was identified as an area where the superior vena cava meets the right atrial appendage. The whole area was collected, including the proximal superior vena cava and atrial appendage wall, sectioned parallel to the long axis of the superior vena cava, fixed in 10% formalin, embedded in paraffin blocks, and stained with hematoxylin and eosin according to established protocols [28,29].

2.2.2 Atrioventricular Conduction Tissue

Forty-one AV CCS tissue samples including the AV node, bundle of His, and bundle branches were obtained from the 17 autopsied hearts. The triangle of Koch was identified at the level of the tricuspid valve's septal leaflet, from the coronary sinus entrance including the membranous septum. Then, a block of tissue containing both the interatrial and the interventricular septum around the septal leaflet of the tricuspid valve was collected from each subject, sectioned, fixed in 10% formalin, embedded in paraffin blocks, and stained with hematoxylin and eosin according to established protocols [28,29].

2.3 Histological Staining

In total, 51 histologically approved CCS samples were included. The CCS localization was reviewed by two expert cardiac pathologists (MS, IK) in all the included samples. Once the conduction tissue was confirmed in each block, 5 μm-thick sections were cut from each block. Immunohistochemical staining was done using the Ventana Automatic System (Ventana Medical Systems, Tucson, AZ, USA) and the used antibodies are summarized in Table 1. In addition, Masson's trichrome stained sections (Sigma, Merck Life Science, Espoo, Finland) were used to evaluate the proportions of interstitial collagen, cardiomyocytes, and fat.

Table 1 Summary of used antibodies.

Antigen	Localization	Dilution	Clone	Manufacturer
CD31	pan-endothelial marker	1:100	monoclonal	Dako, Glostrup, Denmark
D2-40 (podoplanin recognizing antibody)	marker of lymphatic endothelium	1:100	monoclonal	Dako, Glostrup, Denmark
S100	general neural marker	1:6000	polyclonal	Dako, Glostrup, Denmark
TH (tyrosine hydroxylase)	marker of sympathetic nerves	1:100	polyclonal	Chemicon, Merck KGaA, Darmstadt, Germany
CHAT (choline acetyltransferase)	marker of parasympathetic nerves	1:300	polyclonal	Chemicon, Merck KGaA, Darmstadt, Germany
GAP43 (growth-associated protein 43)	neural growth marker	1:100	polyclonal	Chemicon, Merck KGaA, Darmstadt, Germany

2.4 Morphometric Analysis

The stained sections were scanned by a NanoZoomer-XR scanner (Hamamatsu Photonics, Hamamatsu, Japan) at 40x magnification. The morphometric analysis was performed by

open-source software for bioimage analysis (QuPath, Queens University, Belfast, Northern Ireland [30]).

The SA node was microscopically identified at the crossing of the SA nodal artery (Fig. 1A). The AV CCS tissue was microscopically identified as the AV node in the atrial portion, the penetrating AV bundle (bundle of His) within the AV membranous septum, and the branching bundle on the crest of the muscular septum forming the proximal parts of the left and right bundle branches (Fig. 1B).

Studied regions of the immunohistochemically stained sections (CD31, D2-40, S100, TH, CHAT, and GAP43) included the CCS tissue, surrounding myocardium, and the non-myocardial fibro-fatty tissue (FFT) containing connective and adipose tissue of the endo- and epicardium. Additionally, regions adjacent to the identified CCS tissue within the expansion radius of 1 mm, 3 mm, and their summary (1+3 mm) were included (Tab. 2, Fig. 1). Only the CCS tissue region was assessed in the Masson's trichrome stained sections to analyze the myocardial collagen, cardiomyocytes, and fat proportions (Fig. 2A, B). The areas of all the upper-mentioned regions were measured in mm^2. The lymphatic and overall vasculature, autonomic innervation, and interstitial collagen were assessed at 20x magnification separately in the selected topographic regions of interest in both the atrial and ventricular regions.

Table 2 Studied regions.

Topographic regions	Abbreviations	Explanatory notes
whole studied area	WSA	WSA = CCS + (1+3mm)
myocardium	Myo	
fibro-fatty tissue	FFT	FFT = (1+3mm) - Myo
cardiac conduction system	CCS	SA node; AV node, bundle of His, branching bundles
1mm radius from CCS	1mm	
3mm radius from CCS	3mm	
1+3mm radius from CCS	1+3mm	

2.5 Interstitial Collagen, Cardiomyocytes, and Fat Quantification

The myocardial collagen, cardiomyocytes, and fat proportions were assessed by a semi-automated approach driven by a machine-learning pixel classifier in Masson trichrome-stained sections. The thresholds were set for blue-stained components to detect collagen, red-stained components to detect cardiomyocytes, and white (unstained) components with an adipocyte-like pattern to detect fatty tissue (Fig. 2). Manual adjustments, such as the exclusion of vessels, perivascular areas, and empty spaces within the tissue were performed. The areas of myocardial collagen, cardiomyocytes, and fat components were measured as a percentage of the CCS region area. A similar approach has been published previously [9].

2.6 Blood and Lymphatic Vasculature Quantification

The areas and densities of CD31- and D2-40- positive vessels were detected by colorimetric thresholding in the DAB (3,3'-diaminobenzidine) channel with the minimum object size set at 15 μm^2. Positively stained structures not related to our study design (e.g. large vessel

endothelium, mesothelial cells, macrophages, some positively stained lymphocytes, and artifacts) were manually excluded based on morphology. The overall and lymphatic vasculature was expressed by the area ($\mu m^2/mm^2$) and number (vessels/mm^2) of vessels per square millimeter of the studied region. The measurements were performed separately for CD31- and D2-40-stained sections. The percentage of lymphatic vasculature was calculated using the following formula: D2-40-positive vessels / CD31-positive vessels *100. The proportion of blood vessels was calculated as subtraction of D2-40-positive vessels from CD31-positive vessels in each studied region.

2.7 Nerve Density Quantification

The autonomic nerve density was quantified as previously described [17,20]. In brief, the positive nerve tissue was manually selected and subsequently quantified by manual counting of nerves per region (nerves/mm^2) and by measuring the nerve tissue area per region ($\mu m^2/mm^2$). The quantification was performed separately for S100-, TH-, CHAT-, and GAP43-stained sections.

2.8 Statistical Analysis

All data are expressed as mean ± standard deviation (SD). The paired comparisons of innervation, vasculature, and collagen among topographical regions were carried out for significance using the Friedman test with post-hoc Wilcoxon test with the Bonferroni correction. Correlation between continuous variables was assessed by Spearman's correlation coefficient (r). Statistical analysis was performed by the Statistical Package for the Social Sciences version 24.0 (SPSS Inc., Chicago, IL, USA). A P-value of < 0.05 was considered significant.

2.9 Ethical Statement

The institutional permissions from both CRY Cardiovascular pathology, Cardiovascular Sciences Research Centre, St. George's University of London UK, and Tampere University, Tampere, Finland, were received. The study was conducted in accordance with the Declaration of Helsinki.

3. Results

The presence of the CCS was microscopically verified in all samples based on the morphology and topography of hematoxylin and eosin and Masson's trichrome-stained sections. No differences in the conduction system morphology were found between male and female subjects. The SA CCS tissue was present around the nodal artery and an indistinct border was identified between the CCS and myocardial cells of the right atrium with prominent interstitial and surrounding collagen. Abundant epicardial fat was observed on the epicardial side of the SA CCS tissue. The AV CCS tissue penetrated from the atria through the membranous part of the interventricular septum. Then the CCS branched on the apex of the muscular part of the septum and was isolated from the myocardium by collagen of the atrioventricular junction.

Results of the overall and lymphatic vasculature, overall innervation, sympathetic and parasympathetic innervation, neural growth, interstitial collagen, cardiomyocytes, and fat proportions of the studied topographic areas are given in detail below. Measurements of

the main differences between atrial and ventricular regions are reported in the text. The topographical differences among studied regions are described and data are graphically presented in Figures 3-5. All measured values are expressed as means ± standard deviation (SD) and *P*-values are shown for both unit types of the measurements.

3.1 Overall, Lymphatic and Blood Vasculature
3.1.1 The Cardiac Conduction System

The mean CD31-positive overall vessel area was 33825.32±24070.72 $\mu m^2/mm^2$ in the SA CCS and 46306.31±13264.85 $\mu m^2/mm^2$ in the AV CCS. The mean CD31-positive overall vessel density was 401.29±328.47 v/mm^2 in the SA CCS and 400.69±136.51 v/mm^2 in the AV CCS (Fig. 3A, B). No significant differences in overall vasculature area or density between the SA and AV CCS were evident (*P*=0.249, *P*=0.753).

The mean blood vessel area was 31084.83±24158.85 $\mu m^2/mm^2$ in the SA CCS and 39742.12±12559.43 $\mu m^2/mm^2$ in the AV CCS. The mean blood vessel density was 397.97±328.56 v/mm^2 in the SA CCS and 391.32±134.23 v/mm^2 in the AV CCS. No statistical differences in blood vessel area and density were observed (*P*=0.600, *P*=0.753).

The D2-40-positive lymphatic vessel area was 2017.45±1563.8 $\mu m^2/mm^2$ in the SA CCS and 6655.82±5928.6 $\mu m^2/mm^2$ in the AV CCS. The D2-40-positive lymphatic vessel density was 2.54±2.04 v/mm^2 in the SA CCS and 10.16±9.02 v/mm^2 in the AV CCS (Fig. 3C, D). Although the lymphatic vessel area did not differ between SA and AV CCS (*P*=0.063), the lymphatic vessel density was significantly decreased in the SA CCS compared to the AV CCS (*P*=0.043). The proportion of lymphatic vessels (% from the CD31-positive vessels in $\mu m^2/mm^2$ and v/mm^2) in the SA CCS accounted for 10.42% and 2.12% of all vessels. Similarly, lymphatic vessels in the AV CCS region formed 13.85% and 5.85% of all vessels. These results suggest slightly enlarged lymphatic vessels in the CCS in terms of the area rather than the number.

3.1.2 Surrounding Tissue

The overall vessel area and density in the atrial region were significantly increased in the atrial myocardium compared to the surrounding fibro-fatty tissue (Fig. 3A). In the ventricular region, the overall vasculature was most abundant in the myocardial tissue in contrast to both the CCS and FFT. Moreover, the overall vasculature was increasing distally to the AV CCS and was lowest in the FFT compared to all the measured regions (Fig. 3B). The blood vessels show the same pattern of distribution in the studied regions as the overall CD31-positive vasculature.

The proportion of lymphatic vessels (% from the CD31-positive vessels in $\mu m^2/mm^2$ and v/mm^2) in the atrial WSA region accounted for 2.71% and 0.59% of all vessels. Moreover, lymphatic vessels in the ventricles formed 2.41% and 0.41% of all vessels in the WSA region. The SA CCS showed significantly increased lymphatic vasculature compared to the surrounding atrial regions, including the myocardium. The atrial myocardium contained markedly sparse lymphatic vessel density that was significantly decreased compared to the FFT (Fig. 3C). Although the lymphatic vasculature was gradually decreasing distally to the SA node, this trend did not reach statistical significance. The AV CCS contained increased lymphatic vessel area and density compared to the adjacent ventricular myocardial tissue. Lymphatic vasculature was significantly increased in the FFT than in the ventricular myocardium. Lymphatic vasculature tended to decrease distally to the AV CCS (Fig. 3D).

8

3.2 Overall and Autonomic Innervation, and Neural Growth

3.2.1 The Cardiac Conduction System

The S100-positive overall nerve density was 20487.2±8545.92 $\mu m^2/mm^2$ (21.72±24.64 n/mm^2) in the SA CCS and 1892.61±1482.75 $\mu m^2/mm^2$ (10.22±9.16 n/mm^2) in the AV CCS (Fig. 4A, B). Significantly increased overall innervation was observed in the SA vs. the AV CCS (P=0.018, P=0.176).

The sympathetic innervation density was 9228.34±4258.93 $\mu m^2/mm^2$ (5.47±3.38 n/mm^2) in the SA and 1729.43±2030.21 $\mu m^2/mm^2$ (10.42±10.79 n/mm^2) in the AV CCS (Fig. 5A, B). The SA CCS showed significantly increased sympathetic innervation compared to the AV CCS (P=0.018, P=0.735). The parasympathetic innervation density was 372.58±482.83 $\mu m^2/mm^2$ (0.23±0.24 n/mm^2) in the SA CCS and 5.64±16.07 $\mu m^2/mm^2$ (0.03±0.1 n/mm^2) in the AV CCS (Fig. 5C, D). No significant difference in parasympathetic innervation was found between the SA and AV CCS (P=0.068, P=0.144). Significantly higher sympathetic innervation was detected in all studied regions within both atrial and ventricular regions including CCS, compared to parasympathetic nerves and ganglia (P<0.05).

The density of nerves with neural growth, detected by GAP43, was 5794.07±5955.22 $\mu m^2/mm^2$ (16.31±13.38 n/mm^2) in the SA CCS and 2138.69±1829.91 $\mu m^2/mm^2$ (10.11±7.74 n/mm^2) in the AV CCS (Fig. 4C, D). The density of nerves with neural growth was significantly higher in the SA CCS compared to the AV CCS (P=0.018, P=0.128).

3.2.2 Surrounding Tissue

The overall nerve density as detected by S100 was significantly increased in the CCS of both the atrial and ventricular regions compared to the surrounding tissue. Moreover, the ventricular FFT showed significantly increased overall innervation than in the myocardium. The overall nerve density was decreasing distally to the AV CCS (Fig. 4A, B).

In the atrial tissue, sympathetic nerve density was significantly increased in the myocardium compared to the FFT. The SA node was not differently innervated by sympathetic nerves than the surrounding atrial tissue (Fig. 5A). The AV CCS, however, showed a significant increase in sympathetic innervation compared to the surrounding tissue (Fig. 5B). Parasympathetic nerve densities were decreased in the CCS and FFT; however, the differences did not reach statistical significance in either atrial or ventricular regions (Fig. 5C, D).

The neural growth density was significantly increased in both the SA node and atrial myocardium compared to the FFT (Fig. 4C). Concerning the ventricular region, the AV CCS showed significantly increased neural growth than both the surrounding myocardium and FFT. The neural growth nerve density tended to decrease distally to the AV CCS (Fig. 4D).

3.3 Collagen, cardiomyocytes, and fat proportions in the cardiac conduction system

The proportion of interstitial collagen in the SA CCS was 54.96±12.12% and the AV CCS was 21.61±10.61%. Although the SA node appeared to be more than two times more fibrotic than the AV CCS tissue, a statistical difference was not reached (P=0.109). The proportion of cardiomyocytes within the SA CCS was 38.75±11.52% and the AV CCS was 71.87±12.89% (P=0.109). The fat proportion was similar in the atrial and ventricular CCS (6.29±1.75% vs. 6.52±4.31%, P=1) (Fig. 2).

9

3.4 Age Correlations with the Cardiac Conduction System Morphology

Sympathetic nerve densities (r=-0.557, *P*=0.02) and neural growth (r=-0.673, *P*=0.003) decreased with age in the AV CCS. Interstitial collagen significantly increased with age only in the SA node (r=0.9, *P*=0.037). Concerning the tissue adjacent to the CCS, overall innervation (r=-0.786, *P*=0.036), lymphatic (r=-0.786, *P*=0.036), and overall vasculature (r=-0.886, *P*=0.019) significantly decreased with age in the atrial myocardium. Additionally, sympathetic nerves decreased with age in the whole ventricular WSA (r=-0.571, *P*=0.017). Overall CD31-positive vessels (r=-0.57, *P*=0.017) decreased with age in the ventricular WSA.

4   Discussion

4.1   Main Findings

The current morphologic and morphometric analysis showed differences in the vasculature, innervation, and collagen in the CCS and surrounding myocardial and fibro-fatty tissue in morphologically normal human hearts. The most important finding was that lymphatic vasculature was increased in the CCS within both atria and ventricles compared to the surrounding tissue, especially the myocardium, where the lymphatic vasculature was substantially lower. The lymphatic vasculature in the SA CCS was lower in comparison to the AV CCS. The overall vasculature was significantly higher in both the atrial and ventricular myocardial tissues than in the FFT. Although the CCS and myocardial overall vasculature showed a similar pattern of distribution in the atria, the overall vessel area and density were significantly lower in the AV CCS. Both the overall and lymphatic vessel areas decreased with age in the atrial myocardium, while only the overall vasculature decreased with age in the ventricular myocardium.

The overall innervation showed increased density in the atria than the ventricles. In addition, both the SA and AV CCS showed increased overall innervation compared to the surrounding regions. The sympathetic nerve density was more predominant than the parasympathetic nerve density in all the atrial and ventricular studied regions. Moreover, the density of sympathetic innervation was higher in the AV CCS than in its surrounding FFT. The neural growth, detected by GAP43, was increased in the SA and AV CCS compared to the surrounding tissue. The overall innervation decreased with age in the atrial myocardium, and sympathetic innervation and neural growth decreased with age in the AV CCS.

Interstitial collagen was around two times higher in the SA CCS than in the AV CCS, but not statistically significant. Additionally, interstitial collagen significantly increased with age in the SA node.

4.2   Vasculature

The blood vasculature in the myocardial tissue is more abundant as compared to the lymphatic vasculature and both systems closely interact [14,15]. The blood vasculature was previously studied in the human SA and AV nodes with conflicting results that the area of CD31-positive vessels was minimal in the CCS tissue (more than 350 blood vessels in each of the nodes) [1]. This discrepancy may be explained by the presence of mainly connective tissue in the CCS. In our series, nearly all the vessels detected by the CD31 immunohistochemistry were blood vessels in the studied regions. The overall vasculature in the AV CCS was lower

than in the ventricular myocardium and higher than in the surrounding FFT. Additionally, the overall vasculature was more abundant in the atrial and ventricular myocardium compared to the surrounding FFT. These observations of blood supply diversity could be attributed to the different energy metabolism in various heart compartments [31].

Several human and animal studies described the lymphatic drainage of the SA node and ventricular CCS [32–36]. The current study used a similar approach for lymphatic vessel quantification as in the previous studies on various human heart compartments [15] and human heart valves [37]. Here, we present that the lymphatic vessel area and density were higher in both SA and AV CCS tissues than in the surrounding non-conduction system tissue. Additionally, the SA CCS lymphatic vessel density was found to be lower compared to the AV CCS, which may be a result of the different lymph flow driving forces between the atria and ventricles. As previously reported, the lymphatic system in the atria is less extensive than in the ventricles and the lymphatic growth may be affected by various pathological conditions [15,38]. A close relationship between the CCS and lymphatic vasculature was demonstrated previously suggesting the clinical impact of lymph flow disturbances on conduction impairment and arrhythmias [3]. A previous study suggested that lymphatic flow resistance is higher in the atria and lymph flow impairment is more frequent in the atria than in the ventricles. Thus lymphatic retention was speculated to induce supraventricular arrhythmias in certain conditions [39]. Similarly, aging, metabolic syndrome, elevated venous pressure, or surgical intervention in the heart area might cause lymphatic dysfunction leading to the development of atrial fibrillation [4]. Hence, further research should be undertaken to investigate the lymphatic and blood vasculature in the CCS under various pathophysiological conditions as it offers potential opportunities for therapeutic interventions.

4.3 Innervation

A previous study demonstrated a decreased innervation density in the CCS related to aging [5]. These results are in agreement with the present findings on reduced sympathetic innervation with age in the whole ventricular studied area and decreased neural growth related to age in the AV CCS. Age-related changes in CCS are clinically relevant, given the ion channels remodeling role that is also associated with heart failure and arrhythmias [40].

The innervation in both SA and AV CCS is complex due to the overlapping distribution of sympathetic and parasympathetic fibers, originating from the stellate ganglion and the right vagal ganglia [2]. The SA and AV CCS are richly innervated by the autonomic nervous system [16] creating direct contact between the autonomic neural tissue and the CCS tissue [5]. Both the morphological proximity and the density of innervation influence the pacemaking activity of the heart [1]. In our study, we showed that the overall innervation was substantially increased in the CCS tissue in comparison to the adjacent studied atrial and ventricular regions, and the atrial tissue contained generally denser innervation than the ventricular tissue. Moreover, the sympathetic innervation and the neural growth were increased in the atrial myocardium compared to the surrounding FFT, as well as in the AV CCS compared to the adjacent areas. These results are in line with previous human and animal studies [5,21–25], which reported abundant innervation of the CCS compared to the adjacent working myocardium. Chow et al. [5] also found a decreasing innervation gradient distally from the

more densely innervated SA node through the rest of the CCS using a semiquantitative assessment of the innervation density.

Several reports have shown dense parasympathetic innervation of both SA and AV CCS in animal hearts using immunohistochemical methods [21,22,25]. On human hearts, however, Kawano et al. [41] showed predominant parasympathetic innervation in the atria and sympathetic innervation in the ventricles. Crick et al. [23] demonstrated in human hearts predominantly parasympathetic innervation in the SA node and AV node, and predominantly sympathetic innervation in the penetrating bundle and the bundle branches. Moreover, higher parasympathetic innervation in the ventricular CCS compared to the ventricular myocardium was previously reported [26]. A more recent study demonstrated that parasympathetic nerves have a significant influence on both atrial and ventricular rate, rhythm, and contractility [42]. Interestingly, we found that the sympathetic nerve density was significantly increased in both SA and AV CCS, myocardium, and FFT compared to parasympathetic innervation, which is a totally new finding. We did not find differences in parasympathetic innervation among the studied regions. This inconsistency could be explained by limited series sizes, individual factors influencing autonomic innervation, or a different methodology (in nerve quantification and different antibodies or clones). Future studies on the cardiac sympathetic and parasympathetic innervation of certain heart areas including the CCS are recommended for its impact on cardiac regulation and involvement in the pathophysiology of several cardiac diseases.

4.4 Myocardial Collagen and Fat

We found out that the SA node contained around two times more collagen than the AV CCS, which may be explained by the fact that the myocytes are encapsulated in the fibrous connective tissue in the SA node [1,2]. Additionally, a previous study suggested that myocardial collagen accumulation leading to fibrotic remodeling is associated with aging [43], which might be connected to the increased prevalence of atrial fibrillation in the elder. The present study reported that interstitial collagen in the SA node significantly increased with age, which is consistent with several studies that reported an increase in fibrosis with aging in the SA node [44–49]. However, these findings do not support the previous study of two hundred normal human hearts, in which collagen content in the SA node did not increase with age [7]. Unlike the SA node, we addressed that the interstitial collagen content did not increase with age in the AV CCS and this finding supports the previous study [45]. However, previous studies have demonstrated an increase in collagen content with aging in the AV CCS [12,47–49]. These inconsistencies may be mainly due to different collagen content measurement approaches.

Myocardium contains a variable amount of fat in physiologic conditions [50]. Fatty replacement of the myocardial tissue was previously studied in association with inflammation in arrhythmogenic right ventricular cardiomyopathy and sudden cardiac death [10,51]. The present study demonstrated a similar fat distribution pattern in both SA and AV CCS (6.3%; 6.5%, respectively) in normal adult hearts. A previous study evaluated the proportion of myocardial fat in the right atrium and right ventricle (4.5%; 7.5%, respectively) with the highest fat amount found in the right ventricular apex samples [52]. Miles et al. [9] reported the fat proportion in the intraventricular septum, right and left ventricle (1.5%; 12.3%; 4.7%, respectively), including epicardial and endocardial layers.

A prior study reported that myocardial fibrosis is more arrhythmogenic than fatty tissue regarding the percentage of nonconductive tissue necessary to induce an arrhythmia [13]. Myocardial collagen and fat accumulation in the CCS might potentially interfere with normal CCS functions and the knowledge of the distribution can contribute to the explanation of CCS pathologies and identifying the cause of death.

4.5 Limitations of the Study

A small number of subjects were included in the study cohort and conclusions may be, therefore, limited. No clinical data were available about the subjects concerning other diseases and pharmacologic therapy, which may have impacted the morphologic patterns of the studied subjects. No genetic testing was done as the included subjects had positive toxicology at the postmortem evaluation. The myocardial collagen, cardiomyocytes, and fat assessment was limited only to the CCS area and was not performed in the surrounding myocardial regions because of extensive artificial empty intramyocardial spaces that would falsely overestimate the fat distribution and affect reproducibility.

5   Conclusions

The present morphologic and morphometric study identified differences in the vasculature, innervation, and collagen distribution within the human CCS. There was increased collagen surrounding the CCS and the interstitial collagen content was twice as much higher in the SA CCS than in the AV CCS. Fat was a normal but minor component of the SA and AV CCS. There were differences in the vasculature, particularly lymphatic vessels were increased in the CCS compared to the surrounding myocardium and connective tissue. There was also an increase in general innervation and neural growth in the CCS compared to the surrounding connective tissue and myocardium which highlights the central role of innervation in the control of the heartbeat. Sympathetic neural dominance was also noted. These differences highlight the unique role of the conduction system with increased collagen protecting the conduction system from the surrounding myocardium. There was increased blood, lymphatic, and nerve supply which means rapid access to blood components and neurotransmitters influencing the specialized cells of the SA and AV CCS tissue, thus controlling the heartbeat. This study sets a morphological benchmark for further morphological investigation of arrhythmias.

Disclosures

None.

References

1. Gómez-Torres FA, Sebastian R, Ruíz-Sauri A. Morphometry and comparative histology of sinus and atrioventricular nodes in humans and pigs and their relevance in the prevention of nodal arrhythmias. Research in Veterinary Science 2020;128:275–285. doi:10.1016/J.RVSC.2019.12.008.

2. Cavero I, Holzgrefe H. Remembering the canonical discoverers of the core components of the mammalian cardiac conduction system: Keith and Flack, Aschoff and Tawara, His, and Purkinje. Advances in Physiology Education 2022;46:549–579. doi:10.1152/advan.00072.2022.

3. Uhley HN, Leeds SE, Sung MA. Lymphatic drainage from the ventricular septum to the atrioventricular node in human beings. Journal of the American College of Cardiology 1983;1:1119–1122. doi:10.1016/S0735-1097(83)80114-4.

4. Lupinski RW, Ryszard Lupinski CW, Lupinski RW. Aortic fat pad and atrial fibrillation: cardiac lymphatics revisited. ANZ Journal of Surgery 2009;79:70–74. doi:10.1111/J.1445-2197.2008.04802.X.

5. Chow LTC, Chow SSM, Anderson RH, Gosling JA. Autonomic innervation of the human cardiac conduction system: Changes from infancy to senility—An immunohistochemical and histochemical analysis. The Anatomical Record 2001;264:169–182. doi:10.1002/AR.1158.

6. González A, Schelbert EB, Díez J, Butler J. Myocardial Interstitial Fibrosis in Heart Failure: Biological and Translational Perspectives. Journal of the American College of Cardiology 2018;71:1696–1706. doi:10.1016/J.JACC.2018.02.021.

7. Bois MC, Wu CW, Martinez CM, Castonguay MC, Jenkins SM, Maleszewski JJ. Age-related histologic features of the sinoatrial node from normal human hearts during the first 10 decades of life: a study of 200 cases. Cardiovascular Pathology 2021;52:107327. doi:10.1016/J.CARPATH.2021.107327.

8. Csepe TA, Kalyanasundaram A, Hansen BJ, Zhao J, Fedorov VV. Fibrosis: a structural modulator of sinoatrial node physiology and dysfunction. Front Physiol 2015;6:37. doi:10.3389/fphys.2015.00037.

9. Miles C, Westaby J, Ster IC, Asimaki A, Boardman P, Joshi A, et al. Morphometric characterization of collagen and fat in normal ventricular myocardium. Cardiovascular Pathology 2020;48:107224. doi:10.1016/j.carpath.2020.107224.

10. Tansey DK, Aly Z, Sheppard MN. Fat in the right ventricle of the normal heart. Histopathology 2005;46:98–104. doi:10.1111/j.1365-2559.2005.02054.x.

11. Bharati S, Lev M. Cardiac conduction system involvement in sudden death of obese young people. American Heart Journal 1995;129:273–281. doi:10.1016/0002-8703(95)90008-X.

12. Michaud K, Romain N, Taroni F, Horisberger B, Mangin P. Evaluation of a simplified method of the conduction system analysis in 110 forensic cases. Forensic Science International 2002;130:13–24. doi:10.1016/S0379-0738(02)00269-4.

13. De Coster T, Claus P, Kazbanov IV, Haemers P, Willems R, Sipido KR, et al. Arrhythmogenicity of fibro-fatty infiltrations. Sci Rep 2018;8:2050. doi:10.1038/s41598-018-20450-w.

14. Ratajska A, Gula G, Flaht-Zabost A, Czarnowska E, Ciszek B, Jankowska-Steifer E, et al. Comparative and developmental anatomy of cardiac lymphatics. The Scientific World Journal 2014;2014. doi:10.1155/2014/183170.

15. Kholová I, Dragneva G, Čermáková P, Laidinen S, Kaskenpää N, Hazes T, et al. Lymphatic vasculature is increased in heart valves, ischaemic and inflamed hearts and in cholesterol-rich and calcified atherosclerotic lesions. European Journal of Clinical Investigation 2011;41:487–497. doi:10.1111/j.1365-2362.2010.02431.x.

16. James TN. Structure and function of the sinus node, AV node and his bundle of the human heart: Part I—Structure. Progress in Cardiovascular Diseases 2002;45:235–267. doi:10.1053/PCAD.2002.130388.

17. Depes D, Mennander A, Paavonen T, Kholová I. Autonomic nerves in myocardial sleeves around caval veins: Potential role in cardiovascular mortality? Cardiovascular Pathology 2022;59:107426. doi:10.1016/J.CARPATH.2022.107426.

18. Chevalier P, Tabib A, Meyronnet D, Chalabreysse L, Restier L, Ludman V, et al. Quantitative study of nerves of the human left atrium. Heart Rhythm 2005;2:518–522. doi:10.1016/j.hrthm.2005.01.022.

19. Petraitiene V, Pauza DH, Benetis R. Distribution of adrenergic and cholinergic nerve fibres within intrinsic nerves at the level of the human heart hilum. European Journal of Cardio-Thoracic Surgery 2014;45:1097–1105. doi:10.1093/ejcts/ezt575.

20. Depes D, Mennander A, Vehniäinen R, Paavonen T, Kholová I. Human Pulmonary Vein Myocardial Sleeve Autonomic Neural Density and Cardiovascular Mortality. Journal of Histochemistry & Cytochemistry 2022;70:627–642. doi:10.1369/00221554221129899.

21. Crick SJ, Sheppard MN, Ho SY, Anderson RH. Localisation and quantitation of autonomic innervation in the porcine heart I: conduction system. Journal of Anatomy 1999;195:341. doi:10.1046/J.1469-7580.1999.19530341.X.

22. Crick SJ, Sheppard MN, Anderson RH, Polak JM, Wharton J. A Quantitative Assessment of Innervation in the Conduction System of the Calf Heart. THE ANATOMICAL RECORD 1996;245:685–698. doi:10.1002/(SICI)1097-0185(199608)245:4.

23. Crick SJ, Wharton J, Sheppard MN, Royston D, Yacoub MH, Anderson RH, et al. Innervation of the human cardiac conduction system. A quantitative immunohistochemical and histochemical study. Circulation 1994;89:1697–1708. doi:10.1161/01.CIR.89.4.1697.

24. Crick SJ, Sheppard' MN, Anderson3 RH, Polak2 JM, Wharton2 J. A quantitative study of nerve distribution in the conduction system of the guinea pig heart. Journal of Anatomy 1996;188:403.

25. Pauza DH, Saburkina I, Rysevaite K, Inokaitis H, Jokubauskas M, Jalife J, et al. Neuroanatomy of the murine cardiac conduction system: A combined stereomicroscopic and fluorescence immunohistochemical study. Autonomic Neuroscience 2013;176:32–47. doi:10.1016/J.AUTNEU.2013.01.006.

26. Kent KM, Epstein SE, Cooper T, Jacobowitz DM. Cholinergic Innervation of the Canine and Human Ventricular Conducting System. Circulation 1974;50:948–955. doi:10.1161/01.CIR.50.5.948.

27. Sheppard MN, Westaby J, Zullo E, Fernandez BVE, Cox S, Cox A. Sudden arrhythmic death and cardiomyopathy are important causes of sudden cardiac death in the UK: results from a national coronial autopsy database. Histopathology 2023. doi:10.1111/his.14889.

28. Sheppard MN. Approach to the cardiac autopsy. Journal of Clinical Pathology 2012;65:484–495. doi:10.1136/JCLINPATH-2011-200366.

29. Sheppard MN. Practical Cardiovascular Pathology. CRC Press; 2022.

30. Bankhead P, Loughrey MB, Fernández JA, Dombrowski Y, McArt DG, Dunne PD, et al. QuPath: Open source software for digital pathology image analysis. Scientific Reports 2017;7:1–7. doi:10.1038/s41598-017-17204-5.

31. Kübler W, Schömig A, Senges J. The conduction and cardiac sympathetic systems: Metabolic aspects. Journal of the American College of Cardiology 1985;5. doi:10.1016/S0735-1097(85)80548-9.

32. Eliska O, Eliskova M. Lymph drainage of sinu-atrial node in man and dog. Acta Anat 1976;96:418–428.

33. Eliska O, Eliskova M. Lymphatic drainage of the ventricular conduction system in man and in the dog. Acta Anatomica 1980;107:205–213. doi:10.1159/000145243.

34. Shimada T, Morita T, Oya M, Kitamura H. Morphological Studies of the Cardiac Lymphatic System. Archives of Histology and Cytology 1990;53:115–126. doi:10.1679/aohc.53.Suppl_115.

35. Shimada T, Noguchi T, Kitamura H, Matsufuji Y, Campbell GR. Structure and distribution of lymphatic capillaries and fenestrated blood capillaries in the conduction system of the rabbit heart. Heart and Vessels 1988;4:123–127. doi:10.1007/BF02058423.

36. Golab B. Lymphatic vessels of the conducting systemof human heart. Folia Morphologica 1977;36:317–322.

37. Niinimäki E, Mennander AA, Paavonen T, Kholová I. Lymphangiogenesis is increased in heart valve endocarditis. International Journal of Cardiology 2016;219:317–321. doi:10.1016/j.ijcard.2016.06.049.

38. Loukas M, Abel N, Shane Tubbs R, Grabska J, Birungi J, Anderson RH. The cardiac lymphatic system. Clinical Anatomy 2011;24:684–691. doi:10.1002/ca.21104.

39. Cui Y. The role of lymphatic vessels in the heart. Pathophysiology 2010;17:307–314. doi:10.1016/j.pathophys.2009.07.006.

40. Boyett MR. 'And the beat goes on' The cardiac conduction system: the wiring system of the heart. Experimental Physiology 2009;94:1035–1049. doi:10.1113/EXPPHYSIOL.2009.046920.

41. Kawano H, Okada R, Yano K. Histological study on the distribution of autonomic nerves in the human heart. Heart and Vessels 2003;18:32–39. doi:10.1007/s003800300005.

42. Coote JH. Myths and realities of the cardiac vagus. The Journal of Physiology 2013;591:4073. doi:10.1113/JPHYSIOL.2013.257758.

43. Horn MA, Trafford AW. Aging and the cardiac collagen matrix: Novel mediators of fibrotic remodelling. Journal of Molecular and Cellular Cardiology 2016;93:175–185. doi:10.1016/J.YJMCC.2015.11.005.

44. Shiraishi I, Takamatsu T, Minamikawa T, Onouchi Z, Fujita S. Quantitative histological analysis of the human sinoatrial node during growth and aging. Circulation 1992;85:2176–2184. doi:10.1161/01.CIR.85.6.2176.

45. Fujino M, Okada R, Arakawa K, Arakawa K. The Relationship of Aging to Histological Changes in the Conduction System of the Normal Human Heart. Japanese Heart Journal 1983;24:13–20. doi:10.1536/IHJ.24.13.

46. Davies MJ, Pomerance From St George A, Middlesex Hospital C. Quantitative study of ageing changes in the human sinoatrial node and internodal tracts. Heart 1972;34:150–152. doi:10.1136/HRT.34.2.150.

47. Comunoglu C, Comunoglu N, Eren B, Tanrıover O, Turkmen N, Gundogmus UN, et al. Age-related histopathological changes in the cardiac conducting system in the Turkish population: an evaluation of 202 autopsy cases. Folia Morphologica 2012;71:178–182.

48. Song Y, Yao Q, Zhu J, Luo B, Liang S. Age-related variation in the interstitial tissues of the cardiac conduction system; and autopsy study of 230 Han Chinese. Forensic Science International 1999;104:133–142. doi:10.1016/S0379-0738(99)00103-6.

49. Song Y, Laaksonen H, Saukko P, Toivonen S, Zhu J. Histopathological findings of cardiac conduction system of 150 Finns. Forensic Science International 2001;119:310–317. doi:10.1016/S0379-0738(00)00457-6.

50. Selthofer-Relatić K, Bošnjak I. Myocardial fat as a part of cardiac visceral adipose tissue: physiological and pathophysiological view. J Endocrinol Invest 2015;38:933–939. doi:10.1007/s40618-015-0258-y.

51. Miles C, Finocchiaro G, Papadakis M, Gray B, Westaby J, Ensam B, et al. Sudden Death and Left Ventricular Involvement in Arrhythmogenic Cardiomyopathy. Circulation 2019;139:1786–1797. doi:10.1161/CIRCULATIONAHA.118.037230.

52. Selthofer-Relatić K, Belovari T, Bijelić N, Kibel A, Rajc J. Presence of Intramyocardial Fat Tissue in the Right Atrium and Right Ventricle – Postmortem Human Analysis. Acta Clin Croat 2018;57:122–129. doi:10.20471/acc.2018.57.01.15.
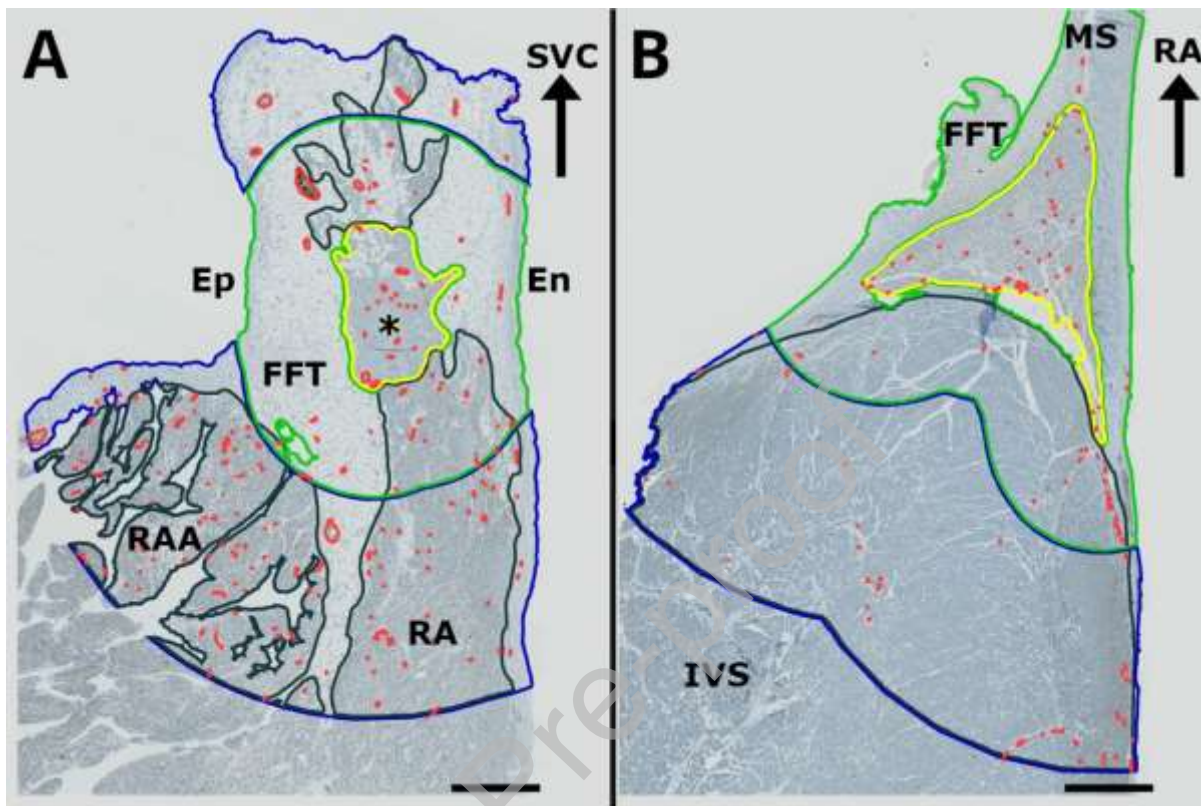
Figure Legends

Figure 1: Studied regions around the sinoatrial and atrioventricular conduction system tissue. A: A histological section of the sinoatrial (SA) node (yellow) adjacent to the SA nodal artery (asterisk). The SA node is located on the subepicardial aspect of the superior vena cava (SVC) and the right atrial appendage (RAA) junction surrounded with abundant fibro-fatty tissue (FFT). B: A histological section of the atrioventricular (AV) conduction system (yellow). After penetrating the membranous portion of the interventricular septum (MS), the AV bundle branches into bundle branches at the crest of the muscular portion of the interventricular septum (IVS), from which they are isolated by the connective tissue. Nerves positive for tyrosine hydroxylase are marked in red and represent sympathetic nerves. Notice the increased sympathetic density in the AV CCS compared to the surrounding tissue. The studied regions: CCS – cardiac conduction system (yellow), myocardium (black), expansion radiuses of 1 mm (green) and 3 mm (blue) from the CCS, and their summary (1+3 mm). Tyrosine hydroxylase stain. Scale bars: 800 μm. Abbreviations: En – endocardium, Ep – epicardium, RA – right atrium.
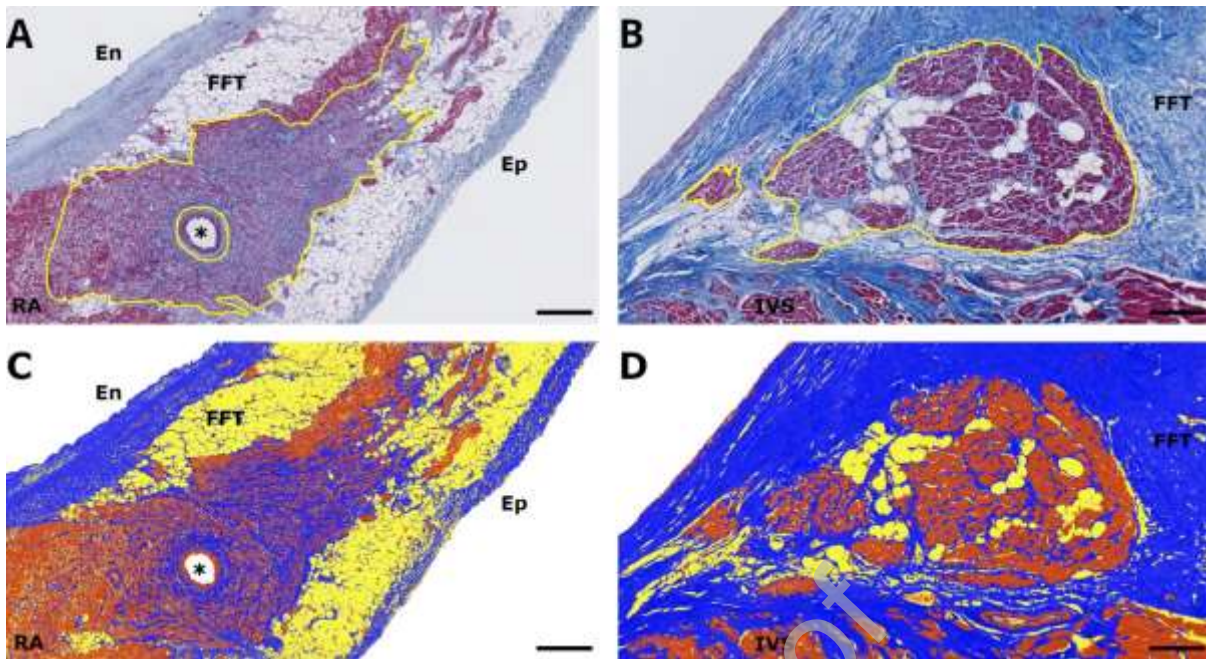
Figure 2: Analysis of the collagen, cardiomyocytes, and fat proportions in the sinoatrial and atrioventricular cardiac conduction system using the pixel classifier. Panels A and B contain colors based on Masson's trichrome stain, where blue=collagen, red=myocardium, and white (unstained)=fat or empty spaces. A: A longitudinal section of the sinoatrial (SA) node (yellow line) with the SA nodal artery (asterisk) surrounded by abundant fibro-fatty tissue (FFT). B: A longitudinal section of the atrioventricular (AV) bundle (yellow line) above the interventricular septum (IVS) and surrounded by the FFT. Panels C and D correspond with panels A and B after the activation of the pixel classifier: blue=collagen, orange=cardiomyocytes, and yellow=fat. C: Corresponds to panel A with activated pixel classifier. Interstitial collagen is noticeably increased in the SA node compared to the surrounding right atrial myocardium. D: Corresponds to panel B with activated pixel classifier. The AV bundle contains numerous adipocytes and adjacent tissue mostly contains collagen. Masson's trichrome stain. Scale bars: A, C=500 µm; B, D=200 µm. Abbreviations: En – endocardium, Ep – epicardium, RA – right atrium.
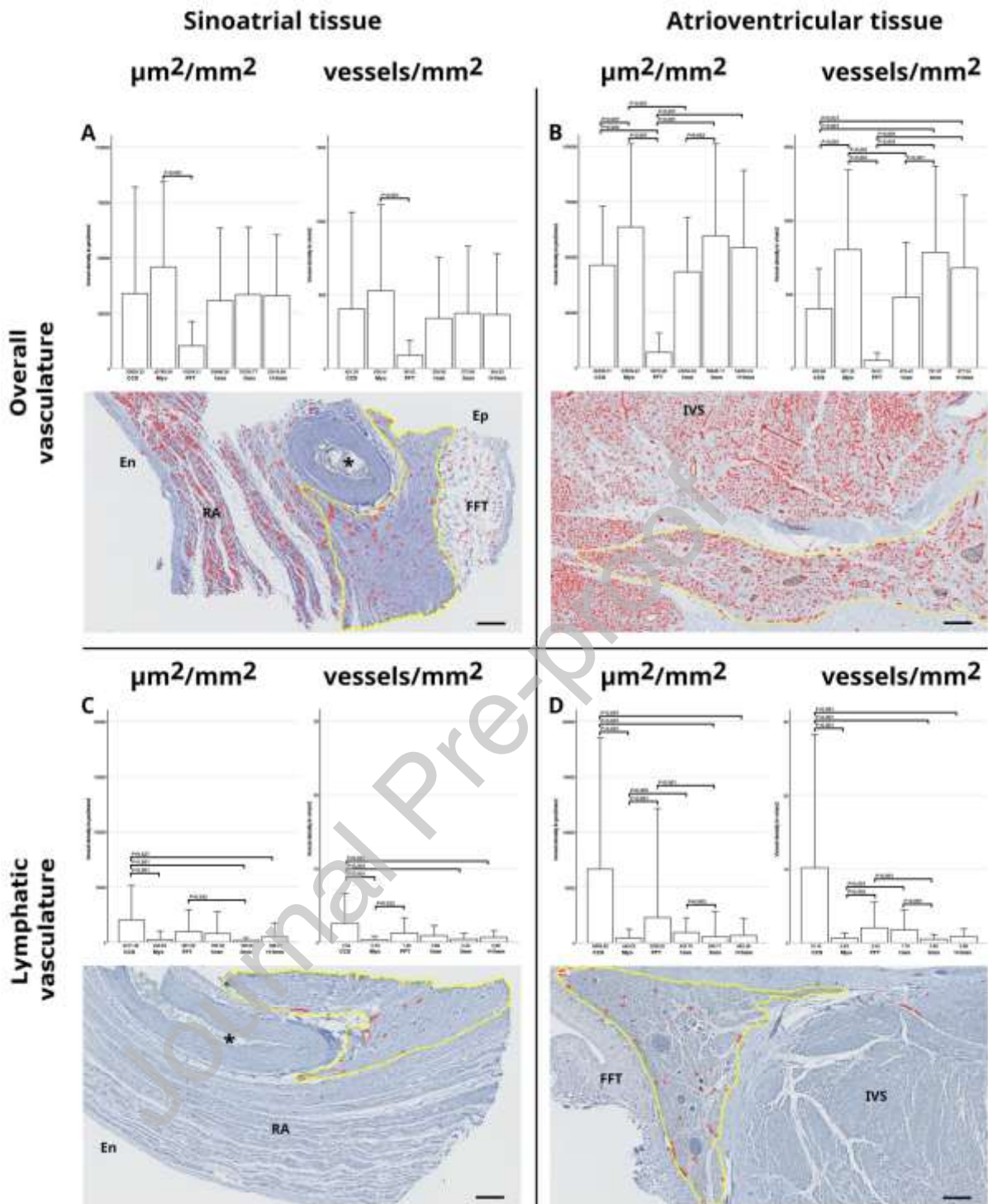
Figure 3: Immunohistochemical analysis of the overall and lymphatic vasculature of the sinoatrial and atrioventricular conduction system tissue and the surrounding regions. The vessel areas and densities were measured in the atrial and ventricular regions and are presented in $\mu m^2/mm^2$ and vessels/mm^2, respectively. Statistically significant differences among the regions ($P < 0.05$) are labeled by bars and their corresponding P-value. The studied regions: CCS – cardiac conduction system, Myo – myocardium, FFT – fibro-fatty tissue, and expansion radiuses of 1 mm and 3 mm from the CCS, and their summary (1+3 mm). The CCS is marked in yellow around the nodal artery (asterisk) in the atrial tissue and on the crest of the muscular portion of the interventricular septum (IVS) in the ventricular

tissue. The positively stained structures corresponding to the used antibodies were annotated in red. A: A section of the sinoatrial (SA) node next to the transversely sectioned nodal artery was surrounded by the myocardium of the right atrium (RA) and fibro-fatty tissue (FFT) on the epicardial aspect. The CD31-positivity was abundant in both CCS and myocardial tissue, and sparse in the FFT. B: The atrioventricular (AV) CCS and the septal myocardium were densely stained with CD31 antibody with less positivity detected in the fibrotic tissue. C: A section of the SA node adjacent to the obliquely sectioned nodal artery was surrounded by the RA myocardial tissue. The D2-40 positivity, representing lymphatic endothelium, was detected mainly in the CCS. D: The AV bundle contained a higher proportion of D2-40-positive lymphatic vessels than the surrounding myocardium. Stains: A, B – CD31 immunohistochemistry (a pan-endothelial marker); C, D – D2-40 immunohistochemistry (a marker of lymphatic vasculature). Scale bars: 250 μm. Abbreviations: En – endocardium, Ep – epicardium, RAA – right atrial appendage.
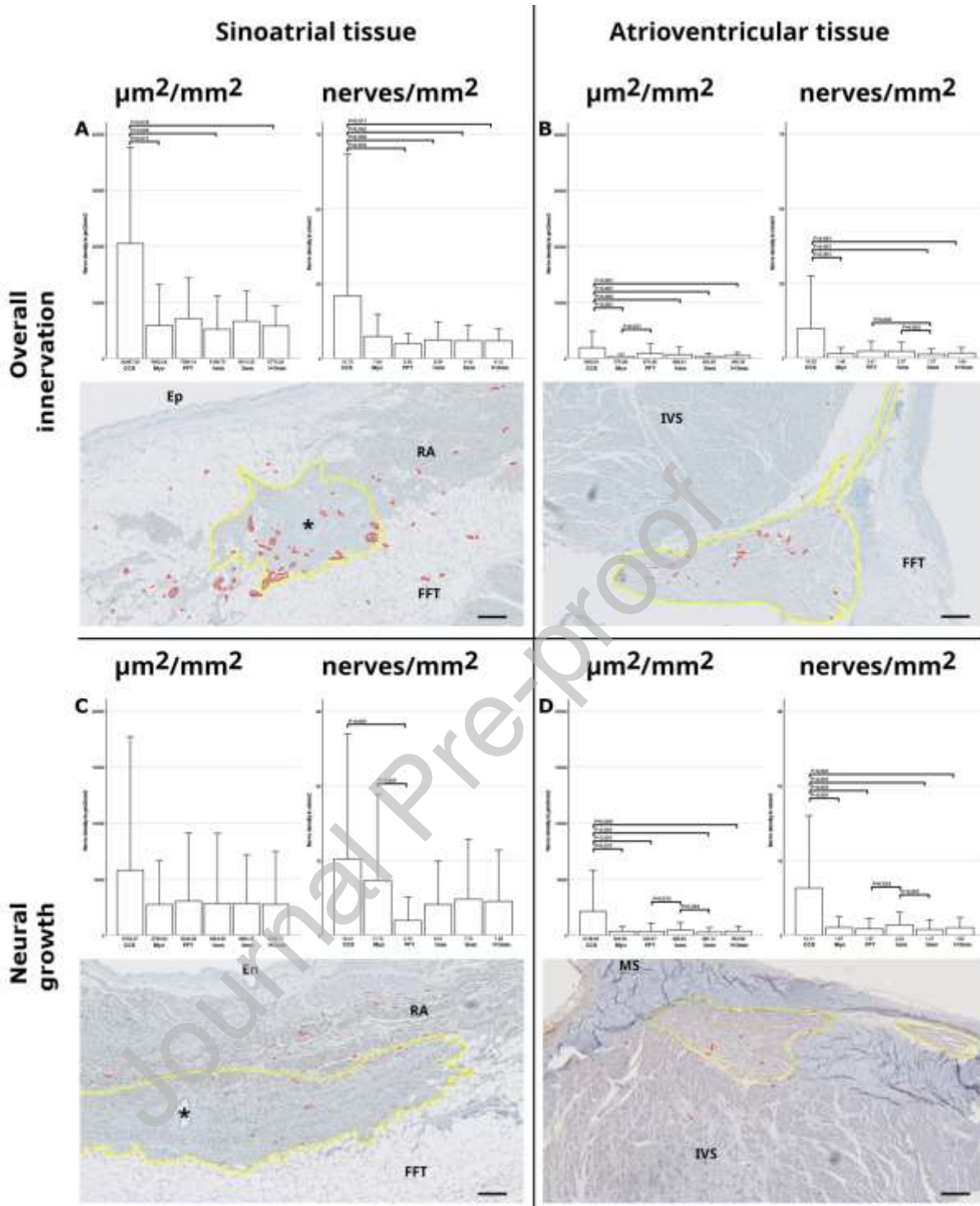
Figure 4: Immunohistochemical analysis of the overall innervation and neural growth densities of the sinoatrial and atrioventricular conduction system tissue and the surrounding regions. The nerve densities are presented in $\mu m^2/mm^2$ and nerves/mm^2. Statistically significant differences among the regions ($P < 0.05$) are labeled by bars and their corresponding *P*-value. The studied regions: CCS – cardiac conduction system, Myo – myocardium, FFT – fibro-fatty tissue, and expansion radiuses of 1 mm and 3 mm from the CCS, and their summary (1+3 mm). The CCS is marked in yellow around the nodal artery (asterisk) in the atrial tissue and on the crest of the muscular portion of the interventricular septum (IVS) in the ventricular tissue. The positively stained structures corresponding to the

used antibodies were annotated in red. A: A transverse section of the sinoatrial (SA) node containing abundant S100-positive nerves. The RA myocardium was partially replaced by fat and surrounded by thick adipose tissue. B: Numerous S100-positive nerves were detected in the branching atrioventricular (AV) CCS surrounded by sparsely innervated septal myocardium and FFT. Both A and B panels show increased overall innervation in the CCS than the surrounding tissue. C: A longitudinal section of the SA node was surrounded by the RA myocardium and FFT. Numerous GAP43-positive nerves were detected in the CCS and RA, but only sporadic in the adipose tissue. D: Dense neural growth was detected in the AV CCS compared to the surrounding tissue. Fibrotic areas were adjacent. The muscular portion of the interventricular septum was slightly fibrotic in the middle part. Stains: A, B – S100 immunohistochemistry (a marker of overall innervation); C, D – growth-associated protein 43 immunohistochemistry (GAP43, a marker of neural growth). Scale bars: 250 µm. Abbreviations: En – endocardium, Ep – epicardium, MS – membranous portion of the interventricular septum.
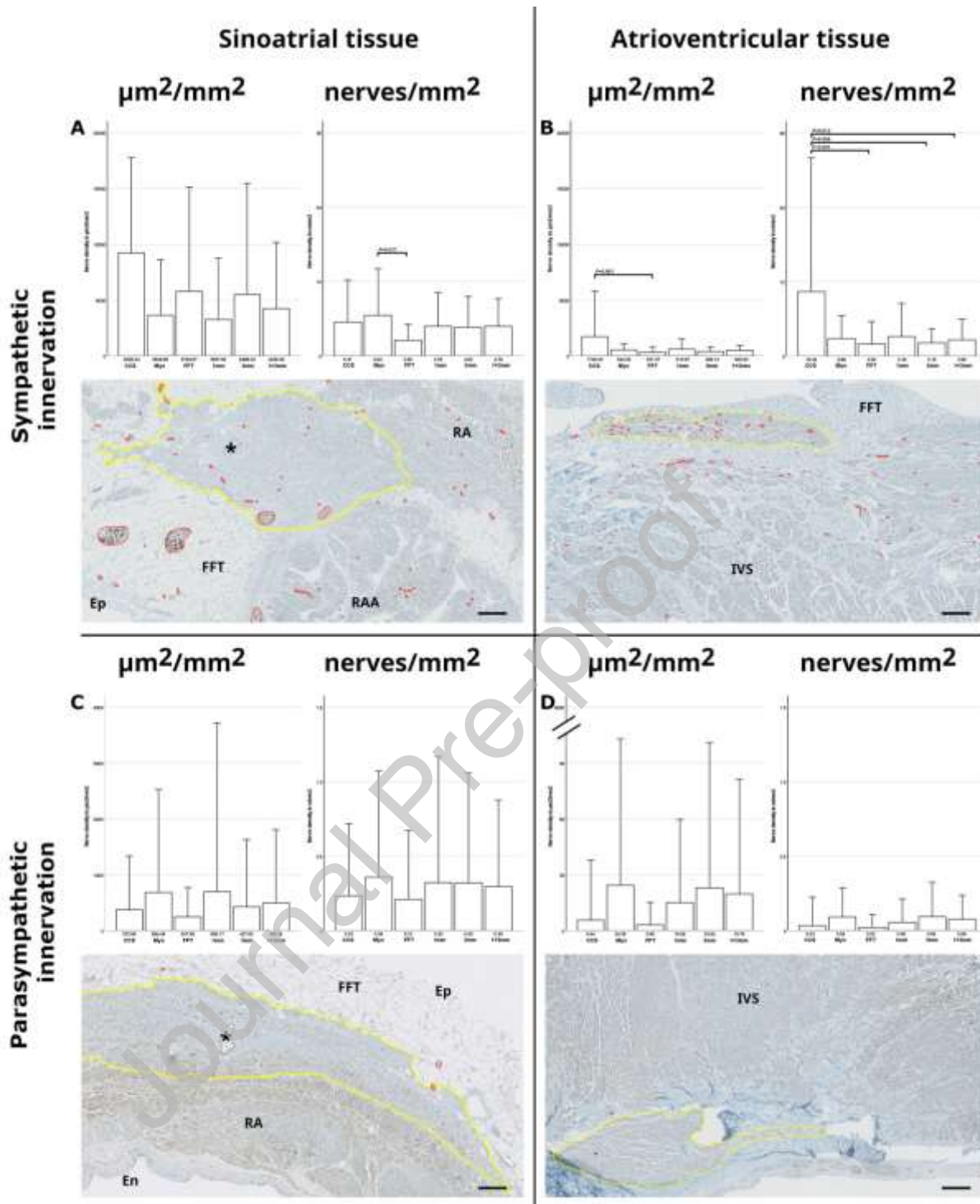
Figure 5: Immunohistochemical analysis of the sympathetic and parasympathetic nerve densities of the sinoatrial and atrioventricular conduction system tissue and the surrounding regions. The nerve densities are presented in $\mu m^2/mm^2$ and nerves/mm^2. Statistically significant differences among the regions ($P < 0.05$) are labeled by bars and their corresponding P-value. The studied regions: CCS – cardiac conduction system, Myo – myocardium, FFT – fibro-fatty tissue, and expansion radiuses of 1 mm and 3 mm from the CCS, and their summary (1+3 mm). The CCS is marked in yellow around the nodal artery (asterisk) in the atrial tissue and on the crest of the muscular portion of the interventricular septum (IVS) in the ventricular tissue. The positively stained structures corresponding to the

used antibodies were annotated in red. A: A transverse section of the SA node around the nodal artery was adjacent to the RA and RAA myocardium with an epicardial abundance of the FFT. The sympathetic nerve density was similar in all the studied regions. B: The AV CCS was densely innervated with sympathetic nerves compared to the surrounding tissue and was separated by connective tissue from moderately fibrotic ventricular myocardium with lower sympathetic innervation. C: A longitudinal section of the SA node was with the RA myocardium on the endocardial part and FFT on the epicardial part. The area contained only sparse parasympathetic nerves. D: A transverse section of the AV CCS and surrounding mildly fibrotic myocardium with only one parasympathetic nerve detected. No differences in parasympathetic innervation were observed within the atria or ventricles. Stains: A, B – tyrosine hydroxylase immunohistochemistry (TH, a marker of sympathetic innervation); C, D – choline acetyltransferase immunohistochemistry (CHAT, a marker of parasympathetic innervation). Scale bars: 250 μm. Abbreviations: En – endocardium, Ep – epicardium, RAA – right atrial appendage.

Graphical Abstract

Detailed Study of Collagen, Vasculature, and Innervation
in the Human Cardiac Conduction System

Aims of the Study

Immunohistochemical and morphometric analysis of the anatomical components in the human cardiac conduction system (CCS).

Materials and Methods

Seventeen human autopsied human hearts (36 ± 16 years) were included. In total, 10 sinoatrial and 17 atrioventricular CCS samples were collected. Immunohistochemical markers were used to assess the densities of vessels, lymphatics, and autonomic nerves. Masson's trichrome stain was used to evaluate interstitial collagen, cardiomyocytes, and fat contents.

Conclusions

Differences in the blood and lymphatic vasculature, autonomic innervation, and collagen distribution within the human CCS were found. These findings make several contributions to the current understanding of the conduction system morphology and provide a deeper insight into the pathophysiology of cardiac arrhythmias and possible further therapeutic interventions.

sinoatrial CCS

atrioventricular CCS
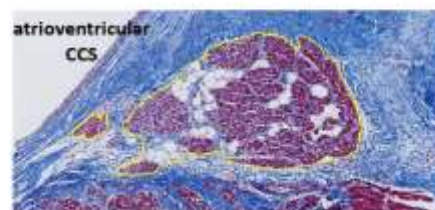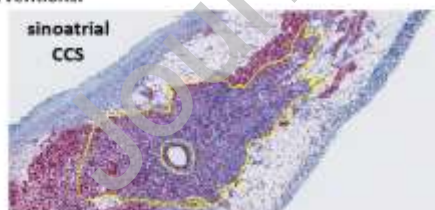
Conflicts of interest: none.

Declaration of interests

☒ The authors declare that they have no known competing financial interests or personal relationships that could have appeared to influence the work reported in this paper.

☐The authors declare the following financial interests/personal relationships which may be considered as potential competing interests: